Hindawi
Geofluids
Volume 2022, Article ID 8430179, 13 pages
https://doi.org/10.1155/2022/8430179

Research Article

Constraints on Diagenetic Fluid Source and Genesis in Tight Dolostone Reservoir of Submember $Ma5_5$ of Ordovician Majiagou Formation in Northwestern Ordos Basin, China: Evidence from Petrology and Geochemistry

Baiqiang Li,[1,2] **Zhenzhen Wu**,[3] **Taofa Zhou**,[1,2] **Bin Chen**,[3] **Qicong Wang**,[3] **and Xiaoli Zhang**[4]

[1]*Ore Deposit and Exploration Centre (ODEC), School of Resources and Environmental Engineering, Hefei University of Technology, Hefei 230009, China*
[2]*Anhui Province Engineering Research Center for Mineral Resources and Mine Environments, Hefei 230009, Anhui, China*
[3]*School of Earth Sciences and Engineering/Shaanxi Key Laboratory of Petroleum Accumulation Geology, Xi'an Shiyou University, Xi'an 710065, China*
[4]*Department of Geology, Northwest University, Xi'an 710069, China*

Correspondence should be addressed to Baiqiang Li; bqli@hfut.edu.cn

Received 18 April 2022; Revised 27 July 2022; Accepted 6 September 2022; Published 18 November 2022

Academic Editor: Fan Yang

Diagenetic fluids is one of the most important reservoir modifiers, their differences can result in various petrography, storage capacity, and geochemical characteristics, so clarifying the diagenetic fluids is vital for understanding dolostone origin. Dolomitization is an important genetic type of dolostone reservoir, the fluid properties differ in different dolomitization, which may lead to reservoir storage capacity changes. Therefore, the identification of dolomitization fluid properties is critical for deeply understanding of dolomitization process and predicting storage capacity. Two types of dolostone are developed in submember $Ma5_5$ of Majiagou Formation in northwestern Ordos Basin, with obviously different petrological characteristics and reservoir properties. On the basis of petrological studies such as core and casting thin section observation and cathodoluminescence analysis, the diagenetic fluid properties of these two dolostone are characterized by geochemical analytical methods such as major and trace element tests. The results show that Type-1 dolostone is mainly composed of micritic dolomite, showing micritic structure and algae-rich lamina structure, and accompanied by evaporite minerals and moldic pores. This type of dolostone has a various Mn content, weak to medium cathodoluminescence intensity, high contents of TiO_2, Al_2O_3, K_2O+Na_2O, Li, and U, and lower content of TFe_2O_3. The type-2 dolostone is composed of fine-grained dolomite with obvious residual texture of primary limestone, clear brim, and cloudy center structure, accompanied by the existence of intergranular pores. Most of this kind of dolostone have medium-strong cathodoluminescence, higher TFe_2O3 content and lower TiO_2, Al_2O_3, K_2O+Na_2O, Li, and U contents. Moreover, both the two types of dolostone have similar Fe/Ca and Mn/Ca ratios, and a low and concentrated CaO content, whose composition is similar to that of stoichiometric dolomite. The comprehensive analysis shows that the diagenetic fluid of Type-1 dolostone is mainly a high salinity fluid existed in plaster and calcareous sediments in a near surface environment with low temperature. The diagenetic fluid of Type-2 dolostone may be a high salinity brine formed by evaporation and concentration of seawater with normal salinity. The research results will provide a significant theoretical basis for the evaluation of dolostone reservoir quality and the prediction of favorable areas of reservoir distribution.

1. Introduction

Carbonate reservoir is of great significance in oil and gas exploration and exploitation; more than 50% of hydrocarbons are produced from these reservoirs globally [1]. Dolostone is one of the most vital gas exploration domains of the Majiagou Formation, Ordos Basin. However, in most cases, carbonate reservoirs have strong heterogeneity in terms of their lithologies and pore structures [2–6]. The influence of diagenesis on reservoir quality has been reported in numerous studies [7–12], among which the differences of diagenetic fluids is one of the most significant controlling factors affecting the formation of effective dolostone reservoirs [13].

Since the formation of tight dolostone reservoir experienced a long-term evolution process, the source and properties of diagenetic fluid are also complicated [13]. At present, although a very high daily gas output of over 1 million cubic meters has been achieved in several industrial gas wells in submember $Ma5_5$, NW Ordos Basin, different opinions on the dolostone formation mechanism of the Member 5 in the Majiagou Formation still remains unclear, one of the reasons is that there is no unified understanding of the diagenetic fluid properties. For example, there is a definite and closed relationship between penecontemporaneous dolomitization fluids and laminar dolomicrite in the northeastern Ordos Basin [14–16] and the central-eastern area [17], but regarding the powder-fine crystalline and medium-crystalline dolomites with a high degree of recrystallization, the source of diagenetic fluids is still up in the air [16], including early mixing of seawater and freshwater [18–20] in the central area, evaporated concentrated brine [21, 22] in the northeastern region [15] and central-eastern area [23–26], seepage reflux dolomitization fluid extensively superimposed by burial dolomitization fluid in late period [22, 27] in the central-eastern area [23, 25, 26, 28], diagenetic dolomitization and burial dolomitization fluids [22, 29], burial dolomitization fluids [30–34] in the northeastern [14, 16] and northwestern areas [35], as well as local hydrothermal dolomitization fluids [36].

Within the entire realm of formation processes related to carbonates, diagenetic fluids is one of the most important reservoir modifiers, different diagenetic fluids can result in various petrography, storage capacity [24], and geochemical characteristics [37, 38], so clarifying the diagenetic fluids is very significant for understanding the dolostone origin.

In view of the above scientific problems, on the basis of drilling core observation, thin section identification, whole rock X-ray diffraction, cathodoluminescence analysis, and other conventional petrological analysis methods, combined with the geochemical analysis of major and trace elements, the main types of dolostone and the properties of diagenetic fluids in submember $Ma5_5$ of Majiagou formation in the northwestern Ordos Basin were studied, and the origin of dolostone were discussed. The research results will provide an important theoretical basis for the evaluation of dolostone reservoir quality and prediction of favorable areas of reservoir distribution.

2. Geologic Setting

During the stratigraphic sedimentary period of the Ordovician Majiagou formation, the Ordos Basin as a whole is a structural pattern alternating between depression and uplift (Figure 1(a)) [39–41]. The central paleo-uplift located in the southwest of the basin and the northern Shaanxi Depression in the east coexist and influence each other for a long time. This tectonic pattern determines the lithofacies palaeogeographic environment of the basin in this period [42]. A set of marine carbonate formations with a stable distribution was deposited in this region during the Early Paleozoic because the basin entered a stable period of craton development [43–45]. According to the characteristics of lithologic changes and sedimentary cycles, the Majiagou formation can be divided into six members from Ma1 to Ma6 from bottom to top, and Member 5 can be divided into 10 submembers from $Ma5_1$ to Ma 5_{10} from top to bottom (Figure 1(b)). Among which, submember $Ma5_5$ is a set of carbonate rocks mainly composed of limestone and dolostone formed in the process of third-order sea level declining and fourth-order sea level rising.

The study area starts from Wuqi in the west to Jingbian in the east, from well S21 in the north to Zhidan in the south. The submember $Ma5_5$ can be divided into three lithologic sections, namely $Ma5_5^1$, $Ma5_5^2$, and $Ma5_5^3$, with a total thickness ranging from 15 to 20 m (Figure 2). A set of dolostone developed in the $Ma5_5^2$ layer formed during a period of fifth-order sea level declining is the object of this study.

3. Materials and Methods

3.1. Samples. The dolostone samples were mainly collected from cores of submember $Ma5_5$ in wells S21, S22, Cc1, Y1112, Y1113, Y1165, Y1117, and D48 in the northwestern Ordos Basin. The well locations and sampling points are shown in Figures 1(a) and 2, respectively. The scope of sampling covers southeastern Wushenqi, western Jingbian, and eastern Wuqi; it almost represents the whole study area. The lithology of the tested samples mainly includes micritic dolomicrite and powder-fine crystalline dolostone.

3.2. Whole Rock X-Ray Diffraction. The volume contents of dolomite, calcite, anhydrite, quartz, and pyrite were determined by whole rock X-ray diffraction analysis. This analysis was completed in the State Engineering Laboratory of low permeability Oil and Gas Field Exploration and Development of Changqing Oilfield Company of China National Petroleum Corporation. The test standard is SY/T 6210-1996 with a data accuracy of 0.01% [25, 26, 47].

3.3. Micropetrography Analysis. The rock structure and pore characteristics in the carbonate rock samples were analyzed through core observations and thin section identification. The number of samples involved in the analysis was nearly 100. Before observing the thin sections, a mixed staining solution containing sodium alizarinsulfonate and potassium ferricyanide was applied, and then, a high power DMLP-217400 microscope was used to identify rock structure and

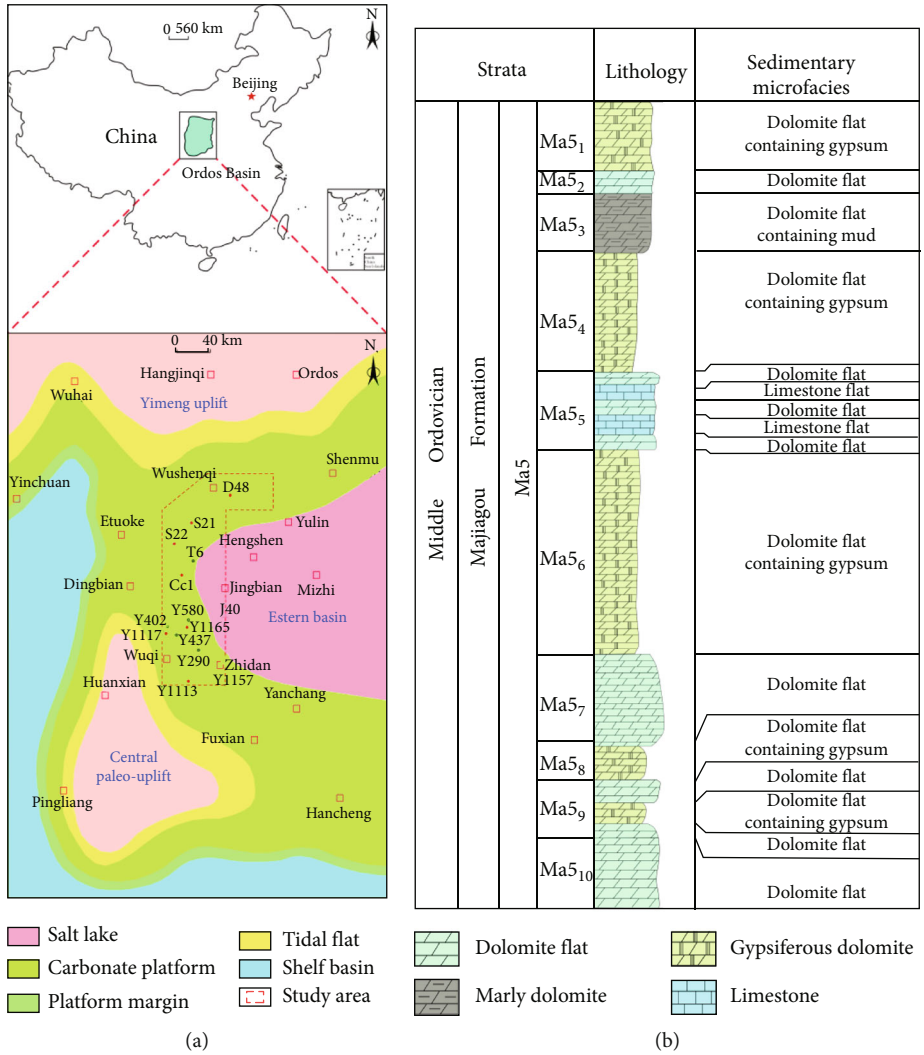

FIGURE 1: (a) Sedimentary environment of the fifth member of the Majiagou Formation in the Ordos Basin and location of the study area (after [46]); (b) comprehensive stratigraphic column of Member Ma5.

pore characteristics. These analyses were conducted at the School of Resources and Environmental Engineering, Hefei University of Technology. The detection standard used was SY/T5368-2000, and all of the samples were analyzed at a room temperature.

3.4. Major and Trace Element Analyses. The testing of magnesium (Mg), calcium (Ca), iron (Fe), manganese (Mn), aluminum (Al), titanium (Ti), sodium (Na), potassium (K), lithium (Li), uranium (U), scandium (Sc), cesium (Cs), and other major and trace elements in the sample were analyzed via inductively coupled plasma mass spectrometry (ICP-MS) at the State Key Laboratory of Marine Geology, Tongji University. The procedure was based on standards DZ/T0223-2001, GB/T 3286.5-1999, and DZG20-05, and the analytical precision of the data is better than 5% [47].

3.5. Electron Probe Microanalysis (EPMA). Electron probe microanalysis was used to excite photons, backscattering electrons, secondary electrons, and X-rays, and to obtain images. The beam spot diameter of the electron probe varies from 0.4 to 1.5 μm. The detected elements included Ca, Mg, Fe, Al, K, Na, Li, U, and other major elements, and Mn, Sr, Ti, Zn, Ba, Ni, S, P, Si, Cl, Br, I, and other trace elements. The brightness of backscattering image strengthens with the increasing of atomic number. The secondary electron images and the X-ray spectrometer are used to show the microscopic features and detect X-rays, respectively, the purpose of the latter is to identify various element components and determine their content.

This test was completed in the State Key Laboratory of Continental Dynamics, Northwest University, using a JEOL JXA-8100 instrument. The analysis was conducted following standard GB/T15616-2008, and the accuracy of the data is 0.001%.

4. Results

4.1. Rock Type and Petrographic Characteristics of Dolostone. According to the genetic-structural classification scheme for carbonate rocks put forward by Feng et al. [48], dolostone in the submember Ma5$_5$ can be divided into Type-1 and Type-

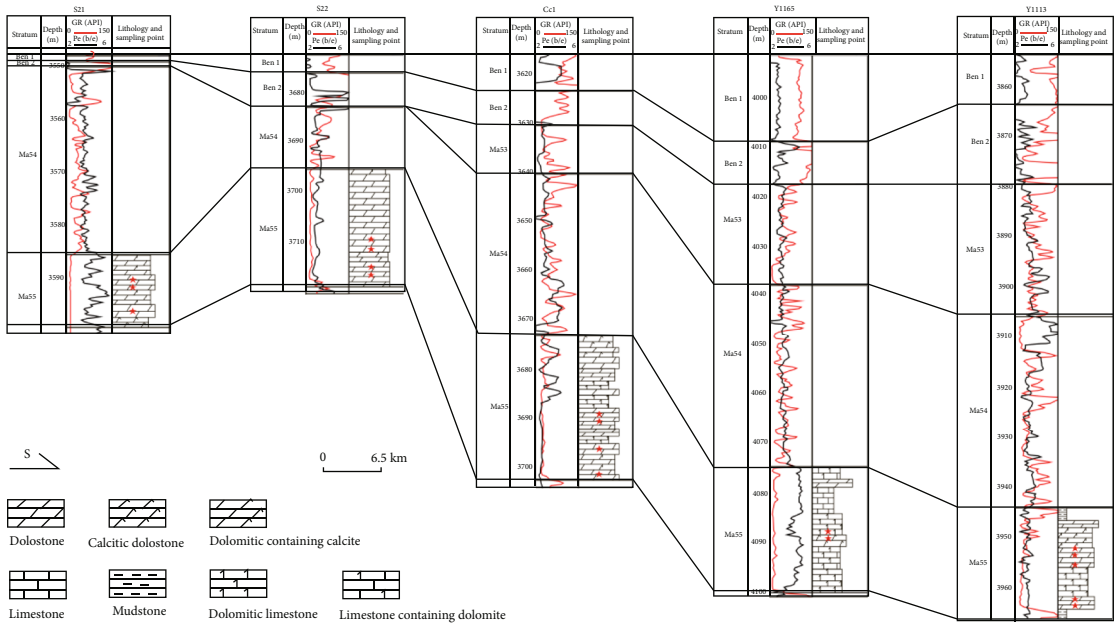

FIGURE 2: Core well section and sampling points of submember $Ma5_5$ in the northwestern Ordos Basin.

2 dolostones, and the specific petrographic characteristics are as follows.

4.1.1. Type-1 Dolostone. Type-1 dolostone is mainly characterized by a dolomite content of greater than 90% and a tight micritic texture. The anhydrite, halite, and other evaporite minerals are common in this kind of dolostone (Figures 3(a) and 3(b)), these minerals usually can be dissolved by surface freshwater to form moldic pores (Figure 3(c)), which is considered to be main pore space of Type-1 dolostone. In addition, some bright and dark laminated algae structures were also observed under plain light (Figure 3(d)).

4.1.2. Type-2 Dolostone. Type-2 dolostone has a dolomite content of greater than 50%, most dolomite exhibits automorphic-hypautomorphic crystals, and the order degree of them varies from 0.7 to 0.85. Under plain light, typical residual texture of primary grainy limestone can be commonly observed (Figure 4(a)), and under cathodoluminescence, cloudy center and clear brim structures (Figure 4(b)) can also be seen in the Type-2 dolostone.

Different from Type-1 dolostone, Type-2 dolostone has better porosity and permeability, this might be contributed to the intercrystalline pores (Figure 4(c)) and some microfractures (Figure 4(d)) developed in this kind of dolostone as they can provide favorable storage space and seepage channels.

4.2. Porosity and Permeability. The measured porosities and permeabilities of nearly 70 samples from submember $Ma5_5$ in the study area are significantly different. The porosity ranges from 1.37% to 14.2%, with a mean of 4.68% (Figure 5(a)), and the permeability varies from 0.004×10^{-3} μm^2 to 11.89×10^{-3} μm^2, with an average value of 1.55×10^{-3} μm^2 (Figure 5(b)). Apart from that, Type-2 dolostone show a relatively better correlation between porosity and permeability than Type-1 dolostone (Figure 5(c)), this may be contributed to the good pore connection of Type-2 dolostone.

4.3. Major and Trace Element Compositions. The major and trace element compositions of dolostone in the study area are shown in Table 1. The MgO content in Type-1 dolostone varies from 11.988% to 19.606%, which is lower than that of Type-2 dolostone (19.771% to 21.075%). CaO concentration of Type-1 dolostone ranges from 25.857% to 39.916%, while that of Type-2 dolostone is between 27.353% and 30.847%. MnO and Fe_2O_{3t} contents of Type-1 dolostone also show relatively lower values (0.004% to 0.009% and 0.203% to 0.721%, respectively) than those of Type-2 dolostone (0.007% to 0.056% and 0.134% to 1.974%. Al_2O_3, TiO_2, Na_2O+K_2O, Li, and U concentrations in Type-1 dolostone are all higher (0.133% to 1.637%, 0.009% to 0.061%, 0.122% to 1.177%, 5.231 to 33.775 ppm, and 1.082 to 1.749 ppm) than those in Type-2 dolostone (0% to 0.042%, 0.002% to 0.006%, 0.066% to 0.100%, 2.556 to 3.955 ppm, and 0.349 to 0.851 ppm, respectively).

5. Discussion

5.1. Element Characteristics of Dolostones. Although the occurrence forms of different major and trace elements in carbonate rocks are diverse, e.g. Fe, Al, K, Sr, Ti, and Mn replace calcium and magnesium ions in calcite or dolomite as isomorphism elements, sodium does not enter the lattice and exists in calcite as a mixture [49], they are sensitive to the changes of diagenetic fluids in carbonate rocks.

In normal seawater environment, Na, I, P, and few Ni, Ba, S, Si, and Al are mainly enriched, while Fe^{2+}, Ti, Mn, Zn, and Br are low. In brine environment with high salinity,

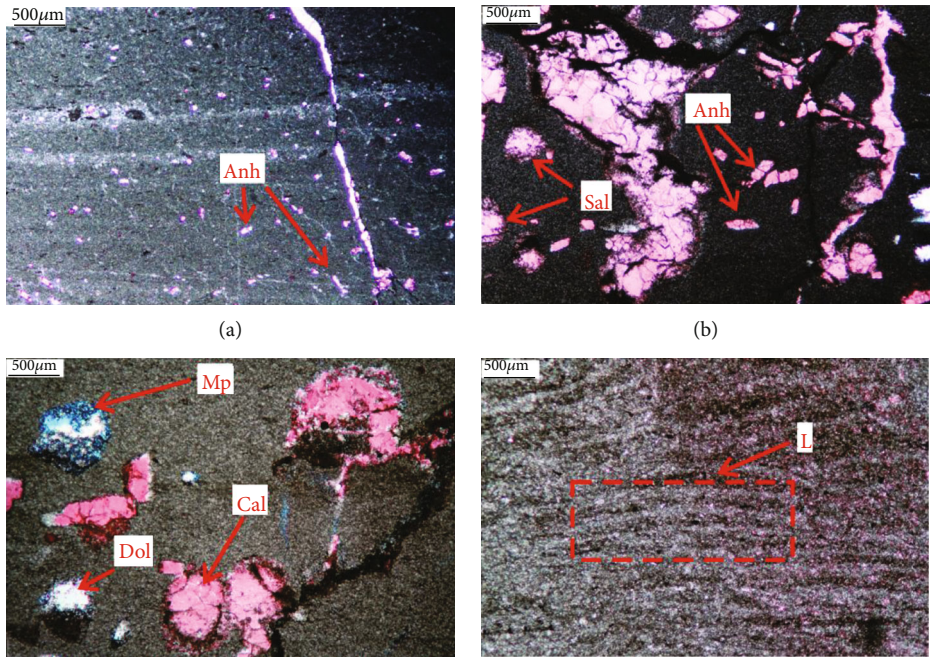

Figure 3: Microphotographs showing the petrographic characteristics of the Type-1 dolostone in Submember $Ma5_5$ in the northwestern Ordos Basin (Anh = anhydrite, Mp = moldic pore, L = laminae, Dol = dolomite, Cal = calcite, and Sal = salt). (a). micritic dolostone, 3107.4 m, well Y1758; (b). salt and anhydrite developed in micritic dolostone, 3859.5 m, well Y1112; (c). moldic pore developed in micritic dolostone, 3860.0 m, well Y1112; (d). laminated structure of stromatolite dolostone, 4089.6 m, well Y1165).

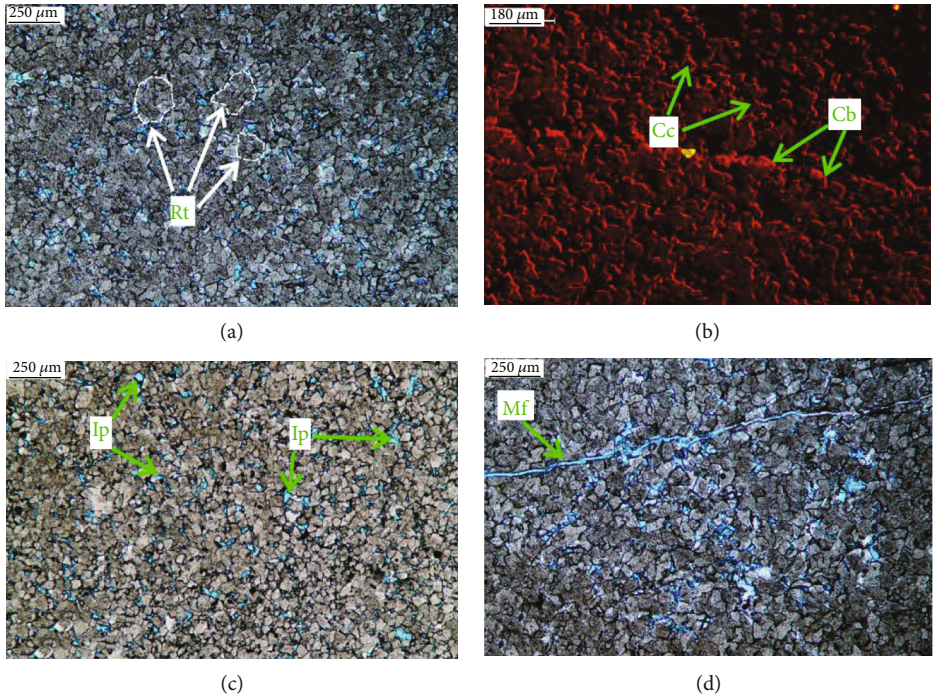

Figure 4: Microphotographs showing the petrographic characteristics of the Type-2 dolostone in submember $Ma5_5$ in the northwestern Ordos Basin (Rt = residual texture; Ip = intercrystalline pore; Cc = cloudy center; Cb = clear brim; and Mf = micro fracture). ((a). Residual texture of the primary limestone developed in the powder-fine crystalline dolostone, 3110.3 m, well Y1758; (b). cloudy center and clear brim textures of the powder-fine crystalline dolostone, 3016.17 m, well D48; (c). intercrystalline pores, 3110.0 m, well Y1758; (d). microfractures in powder-fine crystalline dolostone, 4040.5 m, well Y1117).

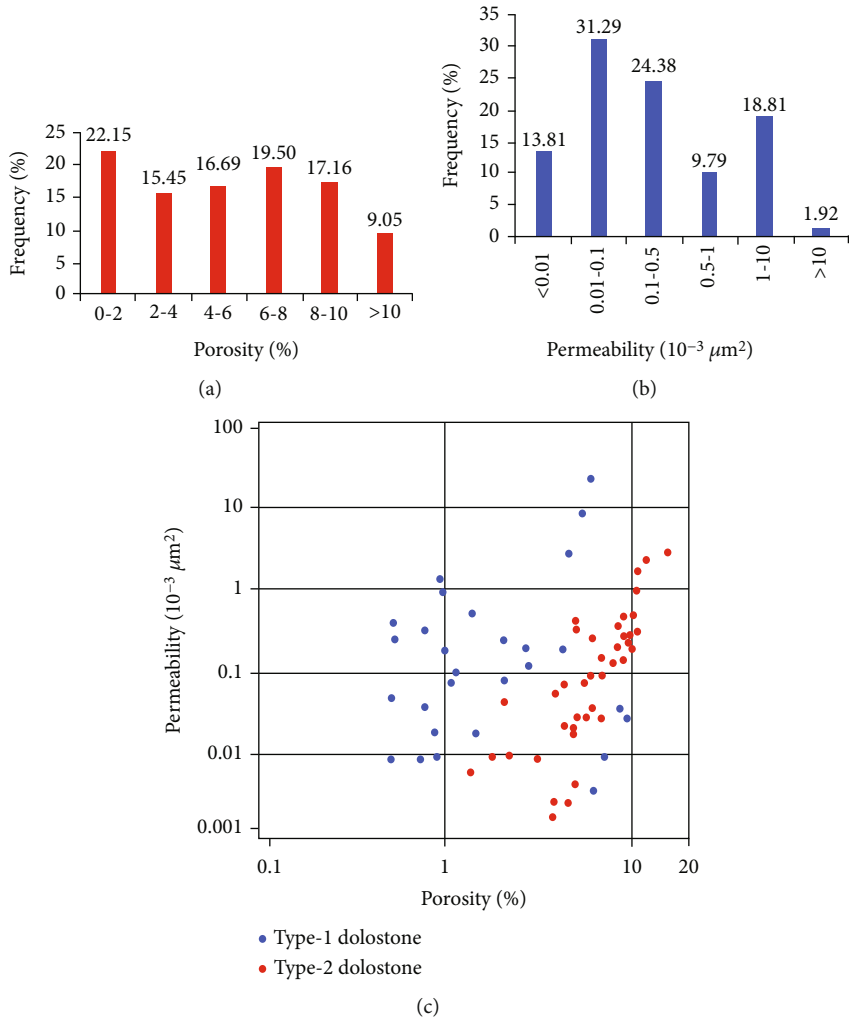

Figure 5: Physical property of dolostone reservoir for submember $Ma5_5$ in the northwestern Ordos Basin. ((a). Frequency distribution of porosity; (b). Frequency distribution of permeabilty; (c). Plot of porosity versus permeability).

Table 1: Element compositions of the dolostones from submember $Ma5_5$ of the Ordovician Majiagou Formation in the northwestern Ordos Basin.

Rock type	Sample number	Na_2O+K_2O (%)	TiO_2 (%)	Al_2O_3 (%)	Fe_2O_{3t} (%)	MnO (%)	MgO (%)	CaO (%)	Mg/ca
Type-1 dolostone	Y1165-4	0.122	0.009	0.133	0.311	0.008	11.988	39.916	0.300
	Y716-1	0.997	0.061	1.385	0.721	0.009	19.606	27.171	0.722
	Y1113-5	0.369	0.023	0.358	0.203	0.004	/	/	/
	Y1113-6	1.177	0.073	1.637	0.441	0.004	19.132	25.857	0.740
Type-2 dolostone	Y1165-3	0.027	0.005	0.000	1.193	0.037	20.568	29.625	0.694
	Y1165-6	0.071	0.004	0.000	0.377	0.011	21.075	30.497	0.691
	Y117-1	0.066	0.006	0.025	1.974	0.056	20.090	27.353	0.734
	Y1112-1	0.100	0.005	0.042	0.254	0.007	19.771	30.847	0.641
	Y1112-4	0.100	0.002	0.000	0.134	0.009	20.027	29.949	0.669

Fe^{2+}, Cl, I, and S are enriched, but as salinity decreases gradually, Fe^{2+}, Na, Cl, Ti, Sr, and S decrease synchronously, while the content of Ba, Zn, Si, and Al increases accordingly. Additionally, Na and P decrease significantly in freshwater environment [23].

5.1.1. Magnesium (mg) and Calcium (ca). According to the relationship between CaO and MgO contents, the CaO contents of most samples are low and concentrated, indicating that all the samples should be metasomatism origin [50]. The compositions of most dolostones are close to that of

stoichiometric dolomite (30.4% CaO and 21.7% MgO) (Figure 6), implying that the metasomatism is relatively high. Apart from that, the ranges of CaO and MgO content ranges (Table 1) reveal that the composition of Type-2 dolostone is closer to that of stoichiometric dolomite than Type-1 dolostone, demonstrating that the metasomatism degree of Type-2 dolostone is higher than that of Type-1 dolostone.

5.1.2. Iron (Fe) and Manganese (Mn). Fe and Mn are the main elements controlling the cathodoluminescence intensity (CI) of carbonate rocks, and freshwater is richer in Fe and Mn contents than seawater [21, 51]. The CI mainly depends on Mn rather than Fe when Mn content is less than 40 ppm, and it has no cathodoluminescence when Mn content is less than 20 ppm. When the Fe content is greater than 5000 ppm, the CI mainly depends on Fe rather than Mn, and it also has no cathodoluminescence when Fe content is greater than 10000 ppm. But when the Mn content is greater than 40 ppm and the Fe content is less than 5000 ppm, the CI generally depends on the Fe/Mn ratio. Specifically, the Fe/Mn>30 corresponds to strong CI (region V), the Fe/Mn<7 corresponds to medium CI (region IV), and intermediate Fe/Mn ratio of 7–30 corresponds to weak CI (region III3) [51, 52].

The plot of Fe versus Mn contents of dolostone in submember $Ma5_5$ and their relationship with the CI [52] (Figure 7) reveal that three Type-1 dolostone samples with relatively low Mn contents are in weak CI regions (region III_1 and III_3), and one sample with a relatively high Mn content is in medium CI region (region IV). This maybe contributed to that the Type-1 dolostone have formed in a near-surface seawater environment and was influenced by atmospheric water because near-surface freshwater is always high in Mn and Fe, and seawater is low in Fe and Mn,

With respect to Type-2 dolostone, three samples have medium CI (region IV) and one sample displays strong CI (region V), this maybe a result of their relative low Fe and high Mn contents in them. Another one exhibits weak CI (region III_2) can be contributed to its high Fe content. These all imply a burial, reducing, and high temperature environment, prompting Mn and Fe to enter the dolomite's crystal lattice [50].

In addition, compared with modern seawater, atmospheric freshwater is richer in Fe and Mn, and the Fe/Ca and Mn/Ca ratios of it are about 1000 times higher than those of modern seawater (Figure 8). In the plot of Fe/Ca versus Mn/Ca, all dolostone samples are close to seawater, and most of them have lower Mn contents than that of modern seawater, indicating that the dolomitization fluids of these samples may have come from Ordovician seawater or a pore fluid equivalent to seawater.

5.1.3. Aluminum (Al), Titanium (Ti), Potassium (K), and Sodium (Na). Al occurs widely in terrigenous clay minerals, its content in illite, kaolinite, and montmorillonite can reach 13.5%, 21%, and 11%, respectively. While in seawater, Al content is low because it always dissolves in strong acid fluids [53]. Ti is one of the relatively stable iron family elements; its content of seawater is very low because it is only soluble in strongly acidic solutions, which rarely exists in natural environment.

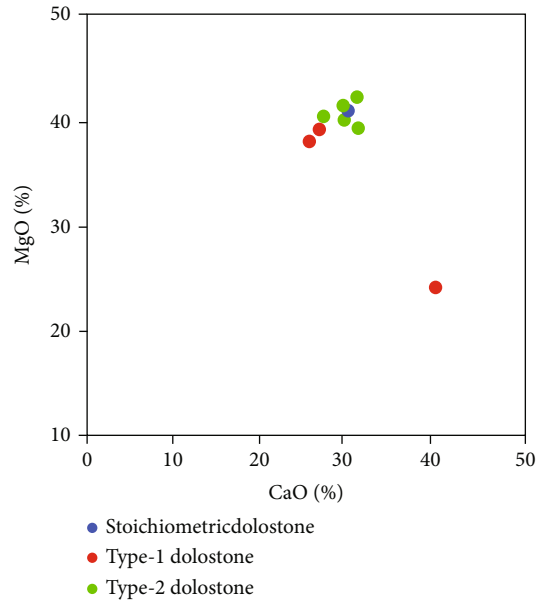

Figure 6: Dolostone compositions and distributions of CaO and MgO contents for submember $Ma5_5$ of the Ordovician Majiagou Formation in the northwestern Ordos Basin.

The decrease of K+Na content is mainly associated with the property of diagenetic fluids rather than the changes in crystalline dolomite during diagenetic processes [54, 55].

Based on the histograms showing the distribution of the major and trace elements, Type-1 dolostone display high TiO_2, Al_2O_3, and K_2O+Na_2O and low Fe_2O_{3t} contents (Figure 9), indicating a high salinity fluid, near-surface, seawater environment [50]. While Type-2 dolostone show high Fe_2O_{3t} and low TiO_2, Al_2O_3, and K_2O+Na_2O contents (Figure 9), implying a burial, high-temperature, and reducing environment, in which the dolomitization accelerated the incorporation of Mn and Fe enter into the dolomite's crystal lattice, reducing the Fe^{3+} to Fe^{2+} [16, 50].

5.1.4. Lithium (Li) and Uranium (U). Since the ionic radii of Fe^{2+} and Mg^{2+} are similar to that of lithium (Li), and Li is easily adsorbed by clay minerals to make it tend to have higher Li contents. With respect to Uranium (U) content, it is very stable in seawater, and generally close to 3.2 ppm. The U content of atmospheric precipitation in the mainland is between 0.01 ppm and 2 ppm, with an average of 0.02 ppm, which is much higher than that over the ocean [56]. In addition, clay minerals also have high U contents because of its strong adsorption capacity [53].

All samples in the study area display a relatively low U contents (less than 2 ppm), this is apparently between the U content in seawater and atmospheric precipitation. In addition, the plot of Li versus U contents shows that the Type-1 dolostone has higher U and Li contents than those of Type-2 dolostone (Figure 10), indicating that Type-1 dolostone was

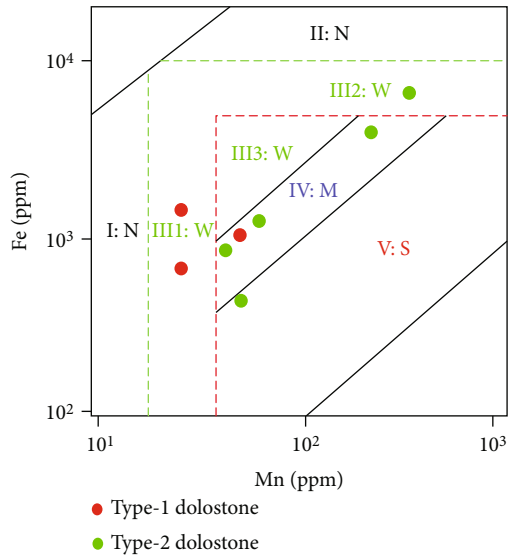

Figure 7: Plot of Mn versus Fe contents for submember $Ma5_5$ of the Ordovician Majiagou Formation in the northwestern Ordos Basin (I, II, III_1, III_2, III_3, IV, and V represent different cathodoluminescence intensity regions. S = strong cathodoluminescence, M = medium cathodoluminescence, W = weak cathodoluminescence, and N = non cathodoluminescence).

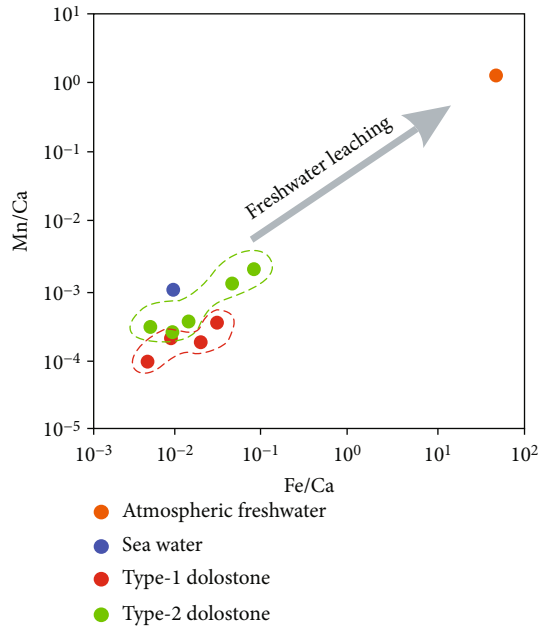

Figure 8: Plot of Mn/Ca versus Fe/Ca for submember $Ma5_5$ of the Ordovician Majiagou Formation in the northwestern Ordos Basin.

influenced by surface freshwater, which carried amount clay minerals to make the Li and U contents increase. In contrast, Type-2 dolostone displays low U and Li contents is mainly contributed to the absence of Li and U sources, indicating that Type-2 dolostone formed in a relatively reducing and enclosed environment.

5.2. Source of Diagenetic Fluids and Genesis of Dolostones

5.2.1. Type-1 Dolostone. Through comprehensive analysis of petrographic and major and trace element characteristics of dolostone, it was found that Type-1 dolostone is mainly composed of micritic dolomite (content of >90%), and it exhibits micritic texture of the primary rock under plain light. The evaporite minerals such as anhydrite and salt coexisting with the micritic dolostone also implicate an evaporative environment, and the presence of moldic pores developed in Type-1 dolostone may demonstrate that atmospheric fresh water is involved in the diagenetic fluid of it.

Three samples are located in weak cathodoluminescence regions have relatively low Mn contents (region III_1 and III_3) and one sample is located in medium cathodoluminescence

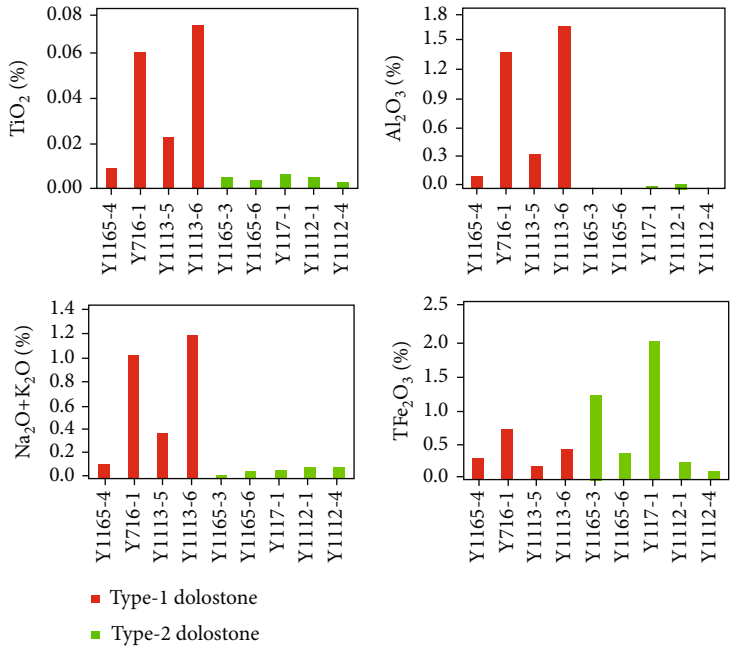

Figure 9: Histograms showing the distributions of the major and trace elements in the different type of dolostones from submember $Ma5_5$ of the Majiagou Formation in the northwestern Ordos Basin.

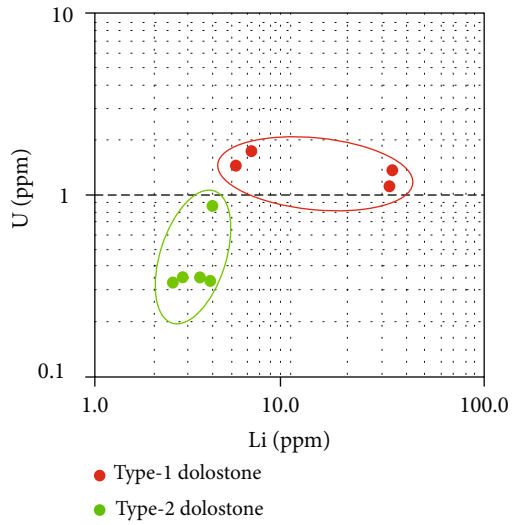

Figure 10: Plot of Li versus U contents for submember $Ma5_5$ of the Ordovician Majiagou Formation in the northwestern Ordos Basin.

region has a relatively high Mn content (region IV) (Figure 7), suggesting diagenetic fluids come from near-surface seawater but were influenced by atmospheric freshwater, which also can be proved by the relationship between Fe/Ca and Mn/Ca ratios (Figure 8).

The high TiO_2 and Al_2O_3 in Type-1 dolostone imply that it formed in a near-surface environment, the high contents of K_2O+Na_2O maybe implicate that the diagenetic fluid of has high salinity, while the low Fe_2O_{3t} content in it demonstrates that the diagenetic fluid is seawater rather than freshwater [50].

The low and concentrated CaO content of most samples is similar to that of stoichiometric dolomite (30.4% CaO and 21.7% MgO), revealing that all of the dolostone samples mainly have a metasomatic genesis [50].

Moreover, Type-1 dolostone has higher U and Li contents than Type-2 dolostone (Figure 10), demonstrating that the former was influenced by surface freshwater [53], which is consistent with the interpretation based on the relationship between Fe/Ca and Mn/Ca ratios.

Based on the above discussion, the diagenetic fluids of Type-1 dolostone can be interpreted as a complex fluids of high-salinity pore fluid and atmospheric freshwater. The genesis of this type of dolostone can be described as follows. During the contemporaneous or penecontemporaneous stage and accompanied by the formation of evaporite minerals resulted from strong evaporation, the salinity of the pore fluid in plaster and calcareous sediments increased, and this type of fluid quickly metasomatized algae-rich aragonite and calcite, then forming micritic dolostone, the high salinity of dolomicrite can also be proved by the result of fluid inclusions data [57]. Through leaching by atmospheric freshwater, the evaporite minerals such as anhydrite and salt dissolved, forming moldic pore. After entering the burial stage, the favorable high-temperature (the homogenization temperature of primary inclusions of dolomicrite is between 82.5 and 138.4°C, and the average value was 112.6°C [57]) and high-pressure conditions furtherly promoted the recrystallization of the micritic dolostone to form a laminated structure.

5.2.2. Type-2 Dolostone. From a petrographic point of view, Type-2 dolostone is mainly composed of powder-fine dolomite, and it exhibits residual texture of the primary rock under plain light. In addition, especially under cathodoluminescence,

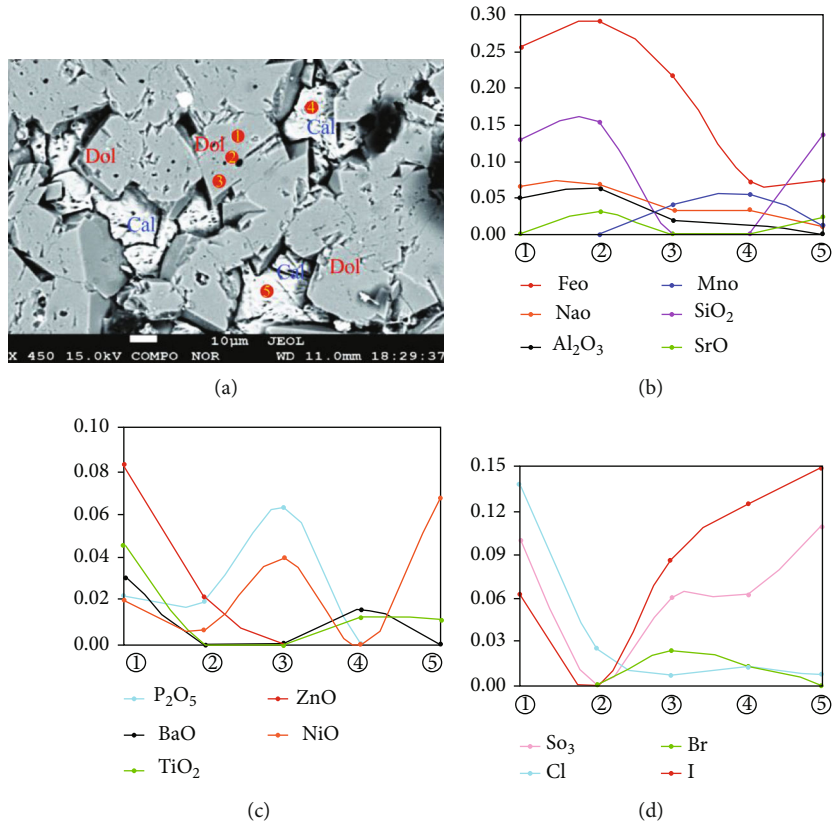

Figure 11: Electron microprobe images and element content variations for the powder-fine dolomite in well D48.

the cloudy centers and clear brims of dolomite are also petrologic evidence of shallow burial active reflux seepage dolomitization because it actually represents the alternation of Mg^{2+} to Ca^{2+} from the nucleus to edge of dolomite crystals. When this dolomitization process is not thorough, part of the limey component will remain in the space between dolomite crystals.

Based on the major and trace element compositions of Type-2 dolostone, the CaO contents of most samples are low and concentrated, indicating metasomatic genesis [50]. The CaO and MgO contents are closer to those of stoichiometric dolomite than those of Type-1 dolostone, indicating that the metasomatism degree of Type-2 dolostone is higher than that of Type-1 dolostone.

With respect to Fe and Mn contents and their relationship with cathodoluminescence, except for one sample with weak cathodoluminescence, most samples have medium-strong cathodoluminescence, implying a burial, reducing, and high temperature environment, which promoted the incorporation of Mn and Fe into the dolomite's crystal lattice [50]. Furthermore, all samples plot in the region close to seawater on the plot of Fe/Ca versus Mn/Ca, also indicates that the diagenetic fluids of Type-2 dolostone may have come from Ordovician seawater or a pore fluid equivalent to seawater.

Apart from the above, the high Fe_2O_{3t}, low TiO_2, Al_2O_3, and K_2O+Na_2O contents also support the opinion that Type-2 dolostone formed in a burial, high temperature, and reducing environment, in which the dolomitization accelerated the incorporation of Fe^{2+} into the dolomite's crystal lattice, reducing the Fe^{3+} to Fe^{2+} [16, 43]. This reducing and enclosed environment also resulted in the low U and Li contents of Type-2 dolostone.

Judging from the EPMA data, the element content changes regularly from the nuclei to edges of dolomite crystal (Figure 11(a)), reflecting the changes of diagenetic environment. As an initial alteration product, the crystal nuclei of powder-fine dolomite has high Fe, Sr, and Na contents, demonstrating a high salinity, reducing environment. It also displays high Si and Al contents, indicating the influence of freshwater (Figure 11(b)). The Cl, Zn, Ti, and Ba contents decrease from the crystal nuclei to the inner zone (Figure 11(c)), while the I, S, P, and Ni contents increase from the inner zone to the outer zone of the dolomite crystals (Figure 11(d)). Undoubtedly, this is the result of a change of diagenetic environment from high salinity to normal salinity fluid, and it also indicates that type of dolostone formed in a shallow and variable salinity seawater environment. The residual limey component between the dolomite crystals has low Si and Al contents and high I, Ni, and S contents, suggesting a normal seawater environment that was influenced by freshwater and formation water in the later period.

From the above analysis of petrology and geochemistry, Type-2 dolostone may have formed in a burial, high temperature (the homogenization temperature of primary inclusions of dolomicrite is between 105.7 and 155.8°C, and the average value was 140.8°C [57]), and reducing environment, and the diagenetic fluids maybe normal seawater but influenced by

freshwater, with a relatively lower salinity (the average salinity of fluid inclusions is nearly 22.6%) than that of Type-1 dolostone (the average salinity of fluid inclusions is nearly 24.2%) [57]. Its formation mechanism can be described as follows. In the early stage, permeable grainy limestone formed in a normal seawater environment, but after the stratum of submember $Ma5_5$ was lifted up and exposed near surface, the seawater began to evaporate and formed Mg^{2+}-rich dolomitization fluid, which refluxed into the underlying grain limestone stratum driven by density and gravity differences. When the stratum was burial again, the formation environment became relatively closed and the temperature increased, and the evaporated seawater was remained in the formation pores, this lead to the pore fluid continued to metasomatize the underlying grainy limestone formation, forming powder-fine crystalline dolostone with residual structure of the primary limestone. But when the dolomitization process was not thorough, some of the limey components could be remained in the spaces between dolomite crystals and were dissolved by the later acidic formation fluids or mixed fluids of seawater and atmospheric freshwater, forming intercrystalline pores and/or intercrystalline dissolution pores.

6. Conclusions

(1) Two types of dolostone were identified in submember $Ma5_5$ of the Ordovician Majiagou Formation in the northwestern Ordos Basin. Type-1 dolostone consists mainly of micritic dolomite, and it is characterized by a micritic texture and an algae-rich laminated structure, associated evaporates minerals and moldic pores. Type-2 dolostone consists of powder-fine crystalline dolomite and is mainly characterized by the residual texture of primary rock, a cloudy center and clear brim texture, and intercrystalline pores

(2) Various Mn content, weak to medium CI, higher contents of TiO_2, Al_2O_3, K_2O+Na_2O, Li, and U, and lower content of Fe_2O_{3t} demonstrate that the diagenetic fluid of Type-1 dolostone is mainly a high salinity fluid existed in plaster and calcareous sediments but was influenced by freshwater, this formed near surface environment with low temperature. Medium-strong CI, higher Fe_2O_{3t} content and lower TiO_2, Al_2O_3, K_2O+Na_2O, Li, and U contents reflect the formation of Type-2 dolostone is related to a high salinity brine, which formed by evaporation and concentration of seawater with normal salinity

Data Availability

All data that support the conclusions of this study are available from the corresponding author upon reasonable request.

Conflicts of Interest

The authors declare that the paper does not have any conflict of interest with other units and individuals.

Acknowledgments

We are grateful to the Geophysics and the State Key Laboratory of Marine Geology, Tongji University, for the major and trace element analyses and to the State Key Laboratory of Continental Dynamics, Northwest University, for the electron microprobe analyses. We also thank the reviewers for their constructive comments and suggestions. This study was supported by the Fundamental Research Funds for the Central Universities (No. JZ2021HGQB0284), the National Natural Science Foundation of China (No. 91962218), the National 13th Five-Year Plan for Science and Technology Major Project of China (No.2017ZX05005-002-004), the Science and Technology Project of Hebei Education Department (No. ZD2022057), and the Natural Science Foundation Research Project of Shaanxi Province (No. 2019JQ-151).

References

[1] L. Jia, C. Cai, L. Jiang, K. Zhang, H. Li, and W. Zhang, "Petrological and geochemical constraints on diagenesis and deep burial dissolution of the Ordovician carbonate reservoirs in the Tazhong area, Tarim Basin, NW China," *Marine and Petroleum Geology*, vol. 78, pp. 271–290, 2016.

[2] C. Hollis, V. Vahrenkamp, S. Tull, A. Mookerjee, C. Taberner, and Y. Huang, "Pore system characterisation in heterogeneous carbonates: an alternative approach to widely-used rock-typing methodologies," *Marine and Petroleum Geology*, vol. 27, no. 4, pp. 772–793, 2010.

[3] J. Lai, S. Wang, C. Zhang et al., "Spectrum of pore types and networks in the deep cambrian to lower ordovician dolostones in Tarim Basin, China," *Marine and Petroleum Geology*, vol. 112, p. 104081, 2020.

[4] C. Matonti, Y. Guglielmi, S. Viseur et al., "Heterogeneities and diagenetic control on the spatial distribution of carbonate rocks acoustic properties at the outcrop scale," *Tectonophysics*, vol. 638, pp. 94–111, 2015.

[5] S. Roth, B. Biswal, G. Afshar et al., "Continuum-based rock model of a reservoir dolostone with four orders of magnitude in pore sizes," *AAPG Bulletin*, vol. 95, no. 6, pp. 925–940, 2011.

[6] B. Q. Wang and I. S. Al-Aasm, "Karst-controlled diagenesis and reservoir development: example from the Ordovician main-reservoir carbonate rocks on the eastern margin of the Ordos Basin, China," *AAPG Bulletin*, vol. 86, pp. 1639–1658, 2002.

[7] G. D. Jones and Y. T. Xiao, "Geothermal convection in the Tengiz carbonate platform, Kazakhstan: reactive transport models of diagenesis and reservoir quality," *AAPG Bulletin*, vol. 90, no. 8, pp. 1251–1272, 2006.

[8] Y. K. Liu, W. Y. He, J. Y. Zhang et al., "Multielement imaging reveals the diagenetic features and varied water redox conditions of a lacustrine dolomite nodule," *Geofluids*, vol. 2022, Article ID 9019061, 20 pages, 2022.

[9] R. G. Maliva, T. M. Missimer, E. A. Clayton, and J. A. D. Dickson, "Diagenesis and porosity preservation in Eocene microporous limestones, South Florida, USA," *Sedimentary Geology*, vol. 217, no. 1-4, pp. 85–94, 2009.

[10] C. H. Moore and W. J. Wade, "Carbonate diagenesis: introduction and tools," *Newnes*, vol. 67, 2013.

[11] M. Paganoni, A. Al Harthi, D. Morad et al., "Impact of stylolitization on diagenesis of a Lower Cretaceous carbonate reservoir from a giant oilfield, Abu Dhabi, United Arab Emirates," *Sedimentary Geology*, vol. 335, pp. 70–92, 2016.

[12] P. Ronchi, A. Ortenzi, O. Borromeo, M. Claps, and W. G. Zempolich, "Depositional setting and diagenetic processes and their impact on the reservoir quality in the late Visean–Bashkirian Kashagan carbonate platform (Pre-Caspian Basin, Kazakhstan)," *AAPG Bulletin*, vol. 94, no. 9, pp. 1313–1348, 2010.

[13] H. P. Bao, F. Yang, Z. H. Cai, Q. P. Wang, and C. Y. Wu, "Origin and reservoir characteristics of Ordovician dolostones in the Ordos Basin," *Natural Gas Industry*, vol. 37, no. 1, pp. 32–46, 2017.

[14] H. Bai, M. Feng, K. F. Hou, T. B. Yang, and S. W. Guo, "Mechanism of dolomite formation in member Ma55 of Majiagou formation, east of Sulige gas field," *Journal of Southwest Petroleum University (Science & Technology Edition)*, vol. 41, no. 4, pp. 65–73, 2019.

[15] C. J. Jiang, X. H. Du, H. Zhang, X. Y. Zhao, and J. G. Wang, "Genesis of dolomite in the lower Ordovician Ma-55 submember in eastern area of Sulige gas field," *Xinjiang Petroleum Geology*, vol. 38, no. 1, pp. 41–48, 2017.

[16] F. J. Li, L. C. Du, J. X. Zhao, Y. G. Li, F. Xiang, and F. P. Li, "Dolomite genesisin member Ma 55 of Majiagou formation, Sudongarea, Ordos Basin," *Acta Petrolei Sinica*, vol. 37, no. 3, pp. 328–338, 2016.

[17] Z. Yu, Z. C. Ding, D. X. Wu, L. B. Wei, and Y. Wei, "Geochemical characteristics and genetic model of dolomite in Majiagou Submember-55 of Ordovician in east-Central Ordos Basin," *Marine Origin Petroleum Geology*, vol. 22, no. 4, pp. 85–93, 2017.

[18] G. R. Li, J. X. Si, and F. Z. Shi, "The types and genetic mechanism of storage space in Ordovician Majiagou formation, Ordos Basin," *Journal of Chengdu University of Technology*, vol. 24, no. 1, pp. 17–23, 1997.

[19] Z. Y. Chen, Z. F. Ma, and J. Q. Zhang, "Genesis of the dolomite in Ma5 Subinterval, Ordivician in central Ordos Basin," *Petroleum Exploration and Development*, vol. 25, no. 6, pp. 20–22, 1998.

[20] J. X. Zhao, H. D. Chen, J. Q. Zhang, X. L. Liu, and S. T. Fu, "Genesis of dolomite in the fifth member of Majiagou formation in the middle Ordos Basin," *Acta Petrolei Sinica*, vol. 26, no. 5, pp. 38–41, 2005.

[21] S. J. Huang, *Diagenesis of Carbonates*, Geological Publishing House, Beijing, 2010.

[22] Z. L. Huang, H. P. Bao, J. F. Ren, H. F. Bai, and C. Y. Wu, "Characteristics and genesis of dolomite in Majiagou formation of Ordovician, south of Ordos Basin," *Geoscience*, vol. 25, no. 5, pp. 925–930, 2011.

[23] Q. C. Wang, W. Wei, J. Zhao et al., "Geochemical characteristics of dolostone diagenetic facies of the Ordovician in Ordos Basin," *Journal of Palaeogeography*, vol. 19, no. 5, pp. 849–864, 2017.

[24] C. Y. Yu and J. P. Cui, "Geochemical characteristics and genesis of dolomite in Majiagou Ma55 submember of the Northeast Yishan Slope, Ordos Basin," *Earth Science*, vol. 44, no. 8, p. 2761, 2019.

[25] B. Q. Li, Q. C. Wang, and X. L. Zhang, "Petrographic and geochemical evidence of the diagenetic environment and fluid source of dolomitization of dolomite: a case study from the Ma55 to Ma51 submembers of the Ordovician Majiagou formation, central Yishan slope, Ordos Basin, China," *Carbonates and Evaporites*, vol. 35, no. 2, p. 36, 2020.

[26] Y. Li, J. H. Yang, Z. J. Pan, and W. S. Tong, "Nanoscale pore structure and mechanical property analysis of coal: an insight combining AFM and SEM images," *Fuel*, vol. 260, p. 116352, 2020.

[27] H. Yang, B. Q. Wang, L. Y. Sun, J. F. Ren, Z. L. Huang, and C. Y. Wu, "Characteristics of oxygen and carbon stable isotopes for middle Ordovician Majiagou formation carbonate rocks in the Ordos Basin," *Natural Gas Geoscience*, vol. 23, no. 4, pp. 616–625, 2012.

[28] B. Q. Li, Q. C. Wang, X. L. Zhang, and W. Wei, "Diagenetic facies and its geochemical characteristics of dolomite: A case study of Ma55-Ma51 Sub-Members of Majiagou Formation in central-eastern Ordos Basin," *Acta Sedimentologica Sinica*, vol. 36, no. 3, pp. 608–616, 2018.

[29] D. L. Liu, X. R. Sun, Z. S. Li, N. A. Tang, Y. Tan, and B. Liu, "Analysis of carbon and oxygen isotope on the Ordovician dolostones in the Ordos Basin," *Petroleum Geology & Experiment*, vol. 28, no. 2, pp. 155–161, 2006.

[30] J. H. Fu, B. Q. Wang, L. Y. Sun, H. P. Bao, and B. Xu, "Dolomitization of Ordovician Majiagou Formation in Sulige region, Ordos Basin," *Petroleum Geology & Experiment*, vol. 33, no. 3, pp. 266–273, 2011.

[31] Z. T. Su, H. D. Chen, F. Y. Xu, L. B. Wei, and J. Li, "Geochemistry and dolomitization mechanism of Majiagou dolomites in Ordovician, Ordos, China," *Acta Petrologica Sinica*, vol. 27, no. 8, pp. 2230–2238, 2011.

[32] B. Q. Wang, Z. T. Qiang, F. Zhang, X. Z. Wang, Y. Wang, and W. Cao, "Isotope characteristics of dolomite from the fifth member of the Ordovician Majiagou formation, the Ordos Basin," *Geochimica*, vol. 38, no. 5, pp. 472–479, 2009.

[33] Y. S. Zhang, "Mechanism of deep burial dolomitization of massive dolostones in the middle Majiagou group of the Ordovician, Ordos Basin," *Acta Sedimentologica Sinica*, vol. 18, no. 3, pp. 424–430, 2000.

[34] W. W. Zhao and B. Q. Wang, "Geochemical characteristics of dolomite from 5th member of the Ordovician Majiagou formation in Sulige area, Ordos Basin," *Acta Geoscientia Sinica*, vol. 32, pp. 681–690, 2011.

[35] X. Zhang, T. S. Zhang, B. J. Lei et al., "Origin and characteristics of grain dolomite of Ordovician Ma_5^5 Member in the northwest of Ordos Basin, NW China," *Petroleum Exploration and Development*, vol. 46, no. 6, pp. 1182–1194, 2019.

[36] J. L. Yao, B. Q. Wang, Y. Wang, D. J. Huang, and C. X. Wen, "Geochemical characteristics of dolomites in lower Ordovician Majiagou formation, Ordos Basin," *Acta Sedimentologica Sinica*, vol. 217, no. 1, pp. 85–94, 2009.

[37] G. D. Jones and Y. T. Xiao, "Dolomitization, anhydrite cementation, and porosity evolution in a reflux system: Insights from reactive transport models," *AAPG Bulletin*, vol. 89, no. 5, pp. 577–601, 2005.

[38] J. Macdonald, C. John, and J. Girard, "Dolomitization processes in hydrocarbon reservoirs: Insight from geothermometry using clumped isotopes," *Procedia Earth and Planetary Science*, vol. 13, pp. 265–268, 2015.

[39] F. H. Hou, S. X. Fang, J. S. Zhao et al., "Depositional environment model of middle Ordovician Majiagou formation in Ordos Basin," *Marine Origin Petroleum Geology*, vol. 7, no. 1, pp. 38–46, 2002.

[40] Y. Li, X. D. Gao, S. Z. Meng et al., "Diagenetic sequences of continuously deposited tight sandstones in various environments: a case study from upper Paleozoic sandstones in the Linxing area, eastern Ordos Basin, China," *AAPG Bulletin*, vol. 103, no. 11, pp. 2757–2783, 2019.

[41] Y. Li, C. Zhang, D. Z. Tang et al., "Coal pore size distributions controlled by the coalification process: an experimental study of coals from the Junggar, Ordos and Qinshui Basins in China," *Fuel*, vol. 206, pp. 352–363, 2017.

[42] Y. Xiong, L. Li, C. X. Wen et al., "Characteristics and genesis of Ordovician Ma51+2 sub-member reservoir in northeastern Ordos Basin," *Oil & Gas Geology*, vol. 37, no. 5, pp. 691–701, 2016.

[43] W. H. Li, Q. Chen, Z. C. Li, R. G. Wang, Y. Wang, and Y. Ma, "Lithofacies palaeogeography of the early Paleozoic in Ordos area," *Journal of Palaeogeography*, vol. 14, no. 1, pp. 85–100, 2012.

[44] J. Q. Qiao, R. Littke, L. Zieger, Z. X. Jiang, and F. Reinhard, "Controls on gas storage characteristics of upper Paleozoic shales from the southeastern Ordos Basin," *Marine and Petroleum Geology*, vol. 117, p. 104377, 2020.

[45] J. Q. Qiao, A. Baniasad, L. Zieger, C. Zhang, Q. Luo, and R. Littke, "Paleo-depositional environment, origin and characteristics of organic matter of the Triassic Chang 7 Member of the Yanchang Formation throughout the mid- western part of the Ordos Basin, China," *International Journal of Coal Geology*, vol. 237, p. 103636, 2021.

[46] B. Jiu, W. H. Huang, N. N. Mu, and Y. Li, "Types and controlling factors of Ordovician paleokarst carbonate reservoirs in the southeastern Ordos Basin, China," *Journal of Petroleum Science and Engineering*, vol. 198, article 108162, 2021.

[47] Y. Li, S. Q. Pan, S. Z. Ning, L. Y. Shao, Z. H. Jing, and Z. S. Wang, "Coal measure metallogeny: metallogenic system and implication for resource and environment," *Science China Earth Sciences*, vol. 65, no. 7, pp. 1211–1228, 2022.

[48] Z. Z. Feng, *Sedimentary Petrology*, Petroleum Industry Press, Beijing, 1994.

[49] Z. T. Qiang, *Carbonate Reservoir Geology*, China University of Petroleum Press, Beijing, 2007.

[50] H. G. Liu, B. Liu, S. L. Wu et al., "The types and origin of the Penglaiba formation dolomite in the Yubei area, Tarim Basin," *Acta Petrologica Sinica*, vol. 33, no. 4, pp. 1233–1242, 2017.

[51] B. J. Pierson, "The control of cathodoluminescence in dolomite by iron and manganese," *Sedimentology*, vol. 28, pp. 601–610, 2010.

[52] S. J. Huang, "Relationship between cathodoluminescence and concentration of iron and manganese in carbonate minerals," *Mineralogy and Petrology*, vol. 12, no. 4, pp. 76–81, 1992.

[53] Y. J. Liu, *Element Geochemistry*, Science Press, Chengdu, 1984.

[54] X. Y. He, J. F. Shou, A. J. Shen et al., "Geochemical characteristics and origin of dolomite: a case study from the middle assemblage of Ordovician Majiagou Formation Member 5 of the west of Jingbian Gas Field, Ordos Basin, North China," *Petroleum Exploration and Development*, vol. 41, no. 3, pp. 417–427, 2014.

[55] J. Zhang, B. M. Zhang, and X. Q. Shan, "Major formation mechanisms and models of marine dolomite in middle and western basin of China," *Geological Bulletin of China*, vol. 36, no. 4, pp. 664–675, 2017.

[56] D. J. Dai, Z. S. Tang, X. T. Chen, and D. F. Li, "U geochemical characteristics and the application of U logging response to oil-gas exploration," *Natural Gas Industry*, vol. 15, no. 5, p. 21, 1995.

[57] C. Y. Yu, Y. M. Jia, Z. L. Ren, Q. C. Wang, and H. J. Ren, "Geochemical characteristics and genesis of the Ma55 dolomite of Ordovician Majiagou Formation in Daniudi area, Ordos Basin," *Marine Origin Petroleum Geology*, vol. 26, no. 4, pp. 375–383, 2021.